VBLUW photometry of emission nebulae

Greve, A.; Genderen, A.M. van

Astron. Astrophys. 174, 243–256 (1987)

ASTRONOMY AND ASTROPHYSICS

VBLUW photometry of emission nebulae *

A. Greve [1] **and A.M. van Genderen** [2]

[1] Institut de Radioastronomie Millimetrique, Voie 10, Domaine Universitaire, F-38406 St. Martin d'Héres, France
[2] Sterrewacht Leiden, Huygens Laboratorium, Wassenaarseweg 78, NL-2300 RA Leiden, The Netherlands

Received April 11, accepted October 21, 1986

Summary. Observed *VBLUW* colours of emission nebulae of the SMC, LMC, and the Orion nebula are reconstructed from published emission line ratios and theoretical H and 2-photon continua. We discuss colour corrections for internal reddening, scattered star light (in particular for the Orion nebula), and stellar backgrounds. The calculations reproduce the observed colours in the $(B-U)/(B-L)$ diagram and indicate a correlation of $(B-U)$ with the [O II] 3727/Hβ line ratios. After a more detailed empirical confirmation, this correlation may eventually be used as a diagnostic indicator of emission nebulae.

We also give colours for a few galactic planetary nebulae, and a tentative interpretation of the measurements.

Key words: photometry – emission nebulae – planetary nebulae

1. Introduction

There are few measurements of emission nebulae (EN) with broad band photometric systems designed for stellar observations. This situation may result from the fact that the interpretation of broad passband colours of EN is not straightforward since the observed fluxes contain radiation from many emission lines, continua, and in some cases also from scattered star light. However, following an earlier publication (Greve and van Genderen, 1982, Paper I) and observations of EN with the *VBLUW* system (Greve et al., 1982), we investigated whether measurements of EN with this system, combined with calculations of colours, can give useful astrophysical information. In the commonly used *VBLUW* colour diagrams (CD) the EN occupy large areas (see Fig. 2), distinctly different from stellar colours but preventing immediate interpretation. We will show that 1) for $(B-U)$, $(B-L)$ the colour corrections for internal reddening and scattered light, if measurements are made sufficiently far from the illuminating star(s), are reasonably small so that intrinsic colours can be derived, 2) the observed distribution of EN in the $(B-U)/(B-L)$ diagram can be reproduced from calculations using observed emission line strengths and theoretical continua, and 3) the colour index $(B-U)$ is correlated with the ratio [O II] 3727/Hβ. With empirical verification, and proper calibration, the correlation $(B-U)$ – [O II] 3727/Hβ may be used as a diagnostic indicator of H II regions (cf. Stasinska, 1980; Pagel et al., 1979; Shaver et al., 1983; Aller, 1984). An advantage of trying to use $(B-U)$ to derive [O II]/Hβ lies in the speed of the measurements: accurate $(B-U)$ values for EN of surface brightness $V_J < 15$ mag/(200″)^2 (i.e. 16″ diaphragm) require integration times of ~ 300 s using the 90 cm Dutch telescope at the European Southern Observatory (ESO), Chile.

We discuss, and present data, for two types of emission nebulae: H II regions of the SMC, LMC, and the Orion nebula (abbreviated EN), and galactic planetary nebulae (PN). *VBLUW* observations of the EN and PN are given in Sect. 2. Using observed emission line ratios and theoretical continua, in Sect. 3 we derive colours of EN, the variation in colour caused by internal reddening, and the influence of scattered star light. For the EN we compare in Sect. 4 the calculations and the observations; in Sect. 5 we derive a correlation $(B-U)$ – [O II] 3727/Hβ. The PN are analyzed in Sect. 6. Other photometric systems (*UBV*, Strömgren, Geneva) are briefly discussed in Sect. 7.

2. *VBLUW* observations of EN, PN

VBLUW observations of EN were made with the Walraven photometer attached to the 90 cm Dutch telescope (ESO, Chile). The diameter of the diaphragm was 16″, i.e. (200″)^2. The photometric data for EN of the SMC, LMC, and the Orion nebula (abbreviated ON) are given in Table 1; for the galactic PN the data are given in Table 2. Earlier observations of EN are reported by Greve et al. (1982), Greve and van Genderen (1985), and Laval et al. (1986). The positions of the observations (Table 1) are indicated in Fig. 1a–1h. The off-set positions of the measurements shown in Fig. 1 were determined from a scaled grid in the eyepiece. At the time of measurements a computer controlled off-set drive was not available; for the ON (Fig. 1h) the largest distances from the Trapezium stars thus correspond with the limits of the grid. The observations of the PN were made at the center, or centered on the central star when visible ($V_J < 15$ mag), and at positions approximately 16″, 32″... displaced from the centers. The data of Tables 1 and 2 are not corrected for reddening; the sky background is subtracted. When using the data in the CDs we assume negligible reddening for the SMC and LMC objects; for the ON we take $A_{V_J} = 0.75$ mag (cf. Goudis, 1982); for the PN we use the extinction values given in Table 2, taken from Pottasch (1984), Gathier (1984), and Gathier et al. (1986). For several cases the observations were made close to stars associated with the EN, PN so that the colours may be contaminated by

Send offprint requests to: A. Greve

* Based on observations collected at ESO, La Silla, Chile

Table 1. *VBLUW* colours (system 1980) of emission nebulae, per $(200'')^2$. Observations Dec. 1980 and Jan. 1983

OBJECT	POS.	V	V-B	B-U	U-W	B-L	VJ
		(log. intensity				)	(mag.)
N 13	1	-2.748	0.136	-0.150	0.110	-0.135	13.7
SMC	2+	-2.984	0.060	-0.103	0.071	-0.080	14.3
N 81 SMC	1*	-2.109	0.214	-0.151	0.112	-0.178	12.1
N 83	1	-3.743	0.177	-0.303	0.188	-0.286	16.2
SMC	2	-3.607	0.353	-0.130	0.265	-0.172	15.9
	3	-4.400	0.302	-0.317	(0.702)	(-0.096)	17.9
	4	-3.772	0.272	-0.252	0.278	-0.246	16.3
	5	-3.791	0.215	-0.205	0.230	-0.136	16.3
	6	-3.794	0.196	-0.106	0.229	-0.239	16.4
N 88 SMC	1*	-2.301	0.402	-0.092	0.140	-0.162	12.6
N 90	1+	-3.878	0.024	0.111	-0.107	-0.049	16.6
SMC	2	-4.100	0.225	-0.422	0.563	-0.389	17.1
	3	-3.773	0.356	-0.394	0.346	-0.402	16.3
N 8	1	-3.479	0.320	-0.484	0.431	-0.422	15.6
LMC	2	-3.112	0.323	-0.420	0.343	-0.376	14.6
N 11E	1	-3.929	0.238	-0.549	0.393	-0.515	16.7
LMC	2	-3.682	0.152	-0.378	0.373	-0.355	16.1
	3	-3.730	0.208	-0.498	0.398	-0.456	16.2
	4	-4.283	0.317	-0.737	0.422	-0.655	17.6
N 59	1	-2.769	0.328	-0.367	0.332	-0.364	13.8
LMC	2	-3.204	0.378	-0.311	0.312	-0.304	14.9
	3	-3.855	0.254	-0.560	0.624	-0.458	16.5
	4	-3.567	0.207	-0.379	0.536	-0.366	15.8
	5	-3.768	0.223	-0.598	0.653	-0.514	16.3
	6	-3.497	0.261	-0.541	0.476	-0.524	15.6
	7	-3.074	0.378	-0.298	0.212	-0.293	14.5
	8	-3.088	0.432	-0.281	0.225	-0.288	14.6
	9	-3.646	0.238	-0.163	0.116	-0.185	16.0
N 159 A	1	-2.648	0.338	-0.145	0.237	-0.161	13.5
LMC	2	-2.642	0.419	-0.302	0.317	-0.307	13.5
	3	-2.773	0.402	-0.233	0.318	-0.250	13.8
N 159	4	-3.504	0.187	-0.465	0.566	-0.420	15.6
LMC	5	-3.016	0.184	-0.199	0.264	-0.170	14.4
	6	-3.354	0.205	-0.239	0.445	-0.187	15.3
	7	-3.352	0.225	-0.380	0.401	-0.328	15.2
	8	-3.410	0.180	-0.354	0.444	-0.319	15.4
	9	-3.468	0.075	-0.296	0.300	-0.253	15.5
	10	-2.733	0.253	-0.246	0.266	-0.217	14.1
	11	-3.221	0.142	-0.276	0.341	-0.234	14.9
	12	-3.473	0.240	-0.287	0.407	-0.254	15.5
	13	-3.114	0.183	-0.164	0.276	-0.143	14.7
	14	-3.412	0.107	-0.385	0.349	-0.320	15.4
	15	-3.514	0.050	-0.483	0.518	-0.431	15.7
	16	-3.242	0.075	-0.254	0.322	-0.219	15.0
	17	-3.110	0.086	-0.326	0.331	-0.284	14.6
	18	-3.450	0.135	-0.319	0.380	-0.269	15.5
	19	-3.190	0.014	-0.083	0.130	-0.072	14.9
N 160A	1	-3.665	0.141	-0.455	0.507	-0.382	16.0
LMC	2	-3.002	0.238	-0.332	0.398	-0.291	14.4
	3	-2.906	0.212	-0.144	0.198	-0.130	14.1
	4	-3.717	0.123	-0.347	0.235	-0.235	16.2
	5	-3.166	0.236	-0.260	0.315	-0.244	14.8
	6	-2.372	0.179	-0.203	0.165	-0.156	12.8
	7	-2.790	0.347	-0.316	0.400	-0.291	13.8
	8	-2.881	0.222	-0.177	0.244	-0.170	14.1
	9	-4.135	0.220	-0.270	0.206	-0.325	17.2
	10	-4.140	0.320	0.060	0.124	-0.035	17.2
	12	-2.846	0.217	-0.165	0.186	-0.163	14.0
	13	-3.909	0.282	-0.534	0.601	-0.470	16.6
	14	-3.284	0.179	-0.296	0.358	-0.254	15.1

Table 1 (continued)

OBJECT	POS.	V	V-B	B-U	U-W	B-L	VJ
		(log. intensity				)	(mag.)
ORION	1	-0.072	0.096	0.039	0.045	-0.007	7.1
NEBULA	2	-1.186	0.284	-0.220	0.166	-0.163	9.8
(M42)	3	-1.185	0.310	-0.269	0.223	-0.200	9.8
	4	-1.333	0.265	-0.271	0.232	-0.201	10.2
	5	-1.395	0.265	-0.276	0.240	-0.201	10.4
	6	-1.054	0.318	-0.214	0.162	-0.160	9.5
	7	-1.165	0.326	-0.252	0.229	-0.187	9.8
	8	-1.226	0.258	-0.269	0.226	-0.200	10.0
	9	-1.270	0.254	-0.246	0.192	-0.175	10.0
	10	-1.344	0.240	-0.248	0.188	-0.173	10.2
	11	-0.869	0.280	-0.192	0.159	-0.137	9.0
	12	-0.887	0.326	-0.266	0.233	-0.197	9.1
	13	-1.035	0.280	-0.302	0.262	-0.228	9.5
	14	-1.215	0.262	-0.292	0.236	-0.217	9.9
	15	-1.406	0.220	-0.273	0.205	-0.196	10.4
	16	-0.170	0.000	-0.077	-0.058	-0.011	7.3
	17	-1.281	0.321	-0.214	0.156	-0.154	10.1
	18	-1.492	0.231	-0.266	0.190	-0.194	10.6
	19	-1.574	0.200	-0.239	0.155	-0.174	10.8
	20	-1.511	0.192	-0.256	0.176	-0.186	10.6
	21	-0.130	0.123	0.054	0.115	-0.008	7.2
	22	-1.410	0.216	-0.215	0.135	-0.156	10.4
	23	-1.740	0.194	-0.219	0.153	-0.148	11.2
	24	-1.777	0.184	-0.254	0.209	-0.176	11.3
	25	-1.847	0.186	-0.212	0.200	-0.146	11.5
	26	-0.713	0.276	-0.098	0.152	-0.062	8.6
	27	-1.069	0.320	-0.257	0.212	-0.186	9.5
	28	-1.154	0.282	-0.321	0.274	-0.238	9.7
	29	-1.420	0.208	-0.352	0.294	-0.265	10.4
	30	-1.552	0.195	-0.350	0.278	-0.261	10.8
	31	-0.954	0.308	-0.241	0.201	-0.176	9.2
	32	-1.131	0.253	-0.266	0.223	-0.187	9.7
	33	-1.453	0.226	-0.285	0.209	-0.208	10.5
	34	-1.619	0.193	-0.269	0.176	-0.190	10.9
	35	-1.821	0.204	-0.255	0.166	-0.170	11.4
	36	-1.266	0.294	-0.211	0.148	-0.162	10.0
	37	-1.187	0.292	-0.258	0.174	-0.191	9.8
	38	-1.254	0.254	-0.276	0.196	-0.198	10.0
	39	-1.197	0.234	-0.302	0.230	-0.209	9.9
	40++	-1.313	0.032	-0.251	0.164	-0.166	10.2

\+ possibly a star (see position in Fig. 2a)
++ possibly influenced by Θ^2 ORI A.
* stellar-like object
The SMC and LMC objects are indicated by the numbers of Henize's catalog (1956)

scattered star light. This in particular is the case for the ON. In Table 3 we give the *VBLUW* colours (not corrected for reddening) of the Trapezium stars; the foreground extinctions (nebular and interstellar) at these stars, derived from the *VBLUW* data, are also given in this table. The observations of the Trapezium stars were made with the 16″ diaphragm, thus the measurements include nebular emission inside the aperture. For θ^1 Ori B we give the colours (Table 3) obtained after subtracting the nebular emission measured at position 30 (Table 1). In the further use of the Trapezium measurements we consider these corrections as unimportant.

Except for a few cases, our observations do not correspond with the EN of which line data are taken to calculate colours (Sect. 3.2). Also, for the common objects the photometric data are not obtained at the positions where the spectroscopic observations were made.

Table 2. *VBLUW* colours (system 1980) of galactic planetary nebulae, per $(200'')^2$. Observations Jan. 1983

OBJET	POS.	V	V-B	B-U	U-W	B-L	VJ	AVJ
		(	log. intensity			)	(mag.	)
IC 418	1*	-0.915	0.085	-0.262	0.218	-0.177	9.2	0.62
	2	-1.332	0.113	-0.244	0.261	-0.215	10.2	
NGC 1535	1*	-1.585	0.273	-0.117	-0.040	-0.155	10.8	0.19
	2	-1.912	0.500	-0.046	0.015	-0.235	11.6	
	3	-2.436	0.702	-0.069	0.035	-0.341	12.9	
NGC 2022	1	-2.408	0.402	-0.046	-0.081	-0.108	12.9	0.81
NGC 2392	1*	-1.246	0.093	-0.115	-0.014	-0.100	10.0	0.34
	2	-1.742	0.483	0.060	0.245	-0.162	11.2	
	3	-2.148	0.691	-0.142	0.211	-0.402	12.2	
NGC 2440	1	-1.496	0.767	-0.210	0.148	-0.374	10.5	0.93
	2	-2.652	0.450	-0.101	0.315	-0.258	13.5	
NGC 3242	1*	-1.112	0.515	-0.111	-0.072	-0.260	9.6	0.28
	2	-1.201	0.588	-0.098	-0.054	-0.303	9.8	
	3	-1.431	0.664	-0.067	-0.009	-0.328	10.3	
	4	-1.794	0.759	-0.094	0.039	-0.382	11.3	
NGC 5189	X	-2.521	0.706	-0.224	0.226	-0.394	13.1	1.24

Position 1: observation at center of nebula, with index * centered on central star. Other observations displaced 16", 32", ... from centers in the direction north, for NGC 3242 in direction north-west.
Position X: see Fig. 1i

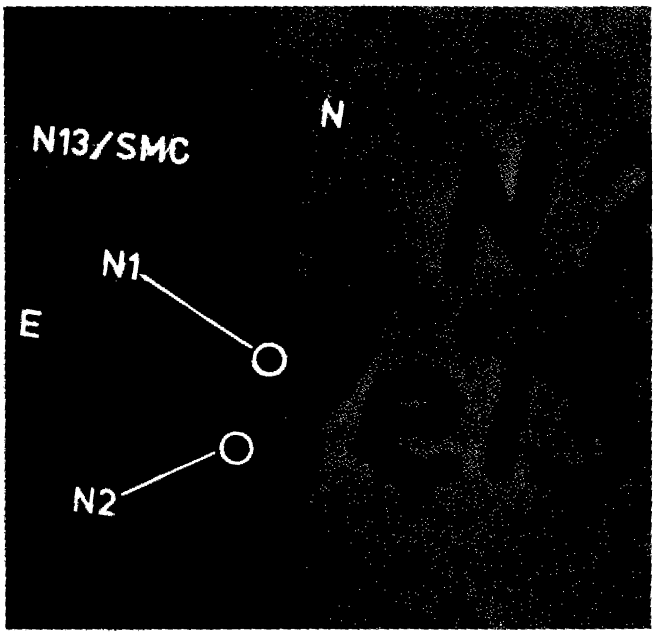

Fig. 1a. N 13/SMC (from Hodge and Wright, 1977). The circles indicate the measurements of the nebular emission; 16″ diaphragm

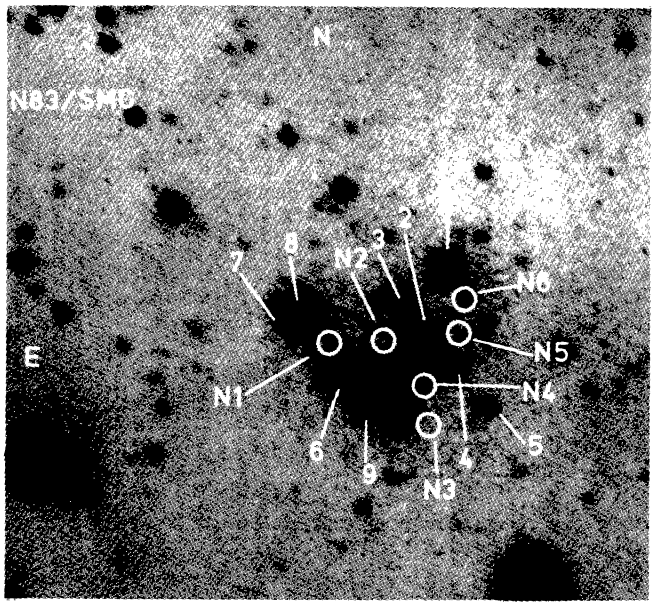

Fig. 1b. N83/SMC (Leiden Atlas). The circles give the positions of the nebular measurements; 16″ diaphragm. The stars, indicated by the numbers, are discussed elsewhere. Similar notation for all other pictures

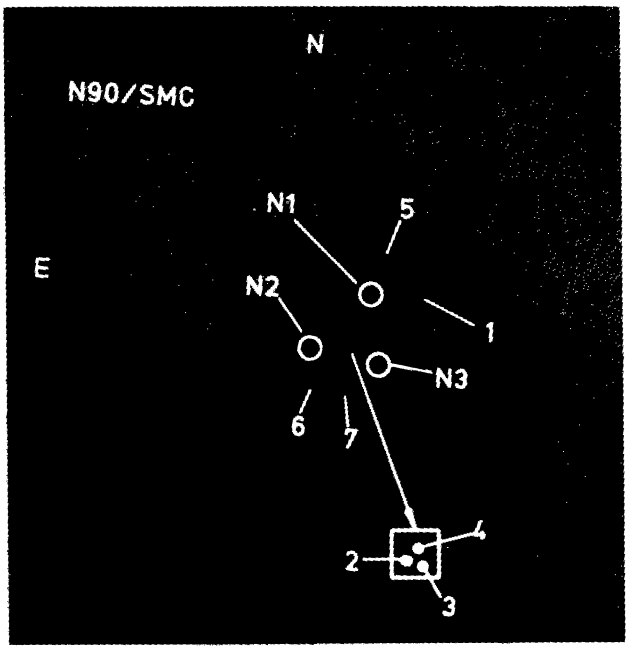

Fig. 1c. N90/SMC (Leiden Atlas)

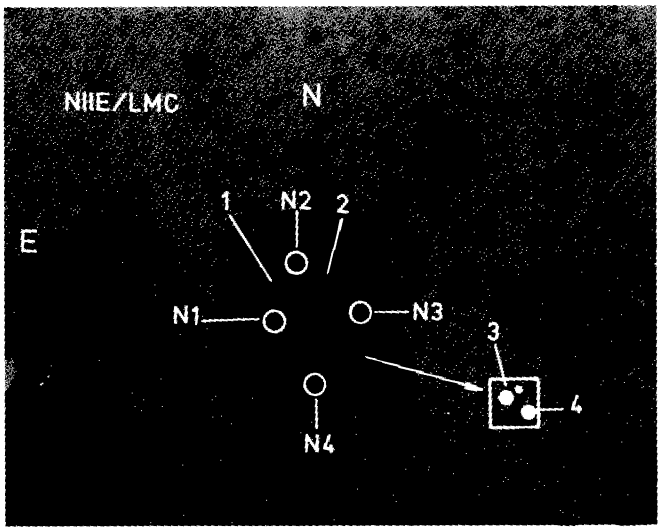

Fig. 1e. N11E/LMC (Leiden Atlas)

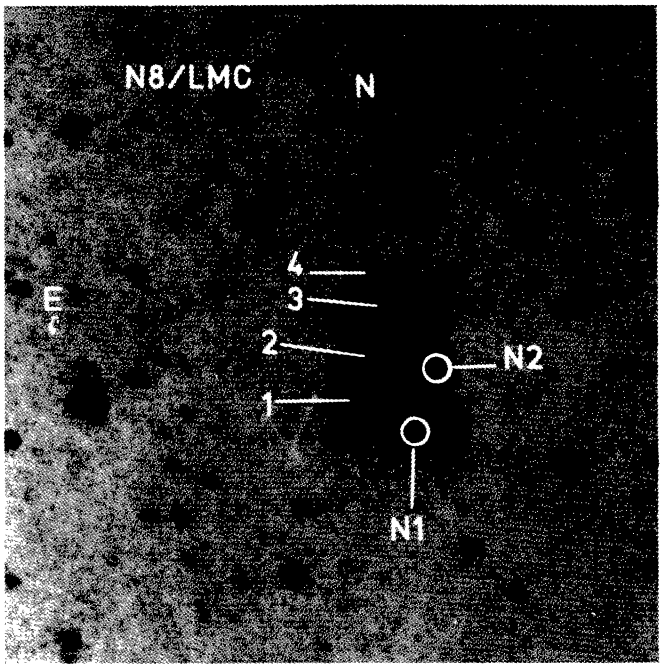

Fig. 1d. N8/LMC (Leiden Atlas)

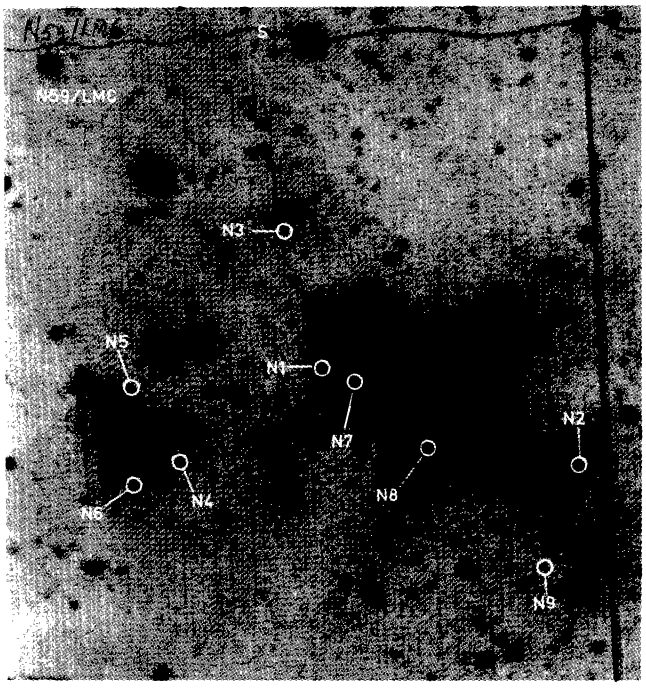

Fig. 1f. N59/LMC (Leiden Atlas)

Table 3. *VBLUW* colours (system 1980) of the Trapezium stars: θ^1 ORI

Star	V	V-B	B-U	U-W	B-L	VJ	AVJ
	(log. intensity				)	(mag.	)
A	0.121	0.052	-0.008	0.001	0.005	6.58	1.25
B	-0.351	0.119	0.086	0.068	0.042	7.75	1.62
B-N(30)	-0.385	0.102	0.134	0.037	0.062	7.82	
C	0.716	0.013	-0.056	-0.019	-0.015	5.09	0.97
D	0.133	0.039	-0.031	-0.003	-0.006	6.55	1.10
ABCD	0.920	0.028	-0.039	-0.011	-0.008	4.59	

The apparent visual magnitudes V_J in the *UBV* system (denoted by the index *J*) given in Tables 1 and 2 are obtained from the relation (Pel, 1983)

$$V_J = 6.889 - 2.5\,[V + 0.039\,(V-B)]. \quad (1)$$

This relation is derived for stars (i.e. quasi continuum sources); for EN the values V_J are accurate within $\sim |0.1|$ mag.

Figures 2a and 2b show the observations of EN (Table 1) and PN (Table 2) in the commonly used CDs. Although the diagrams exhibit considerable scatter, the colours of EN and the nebular part of PN are distinctly different from the colours of the exciting

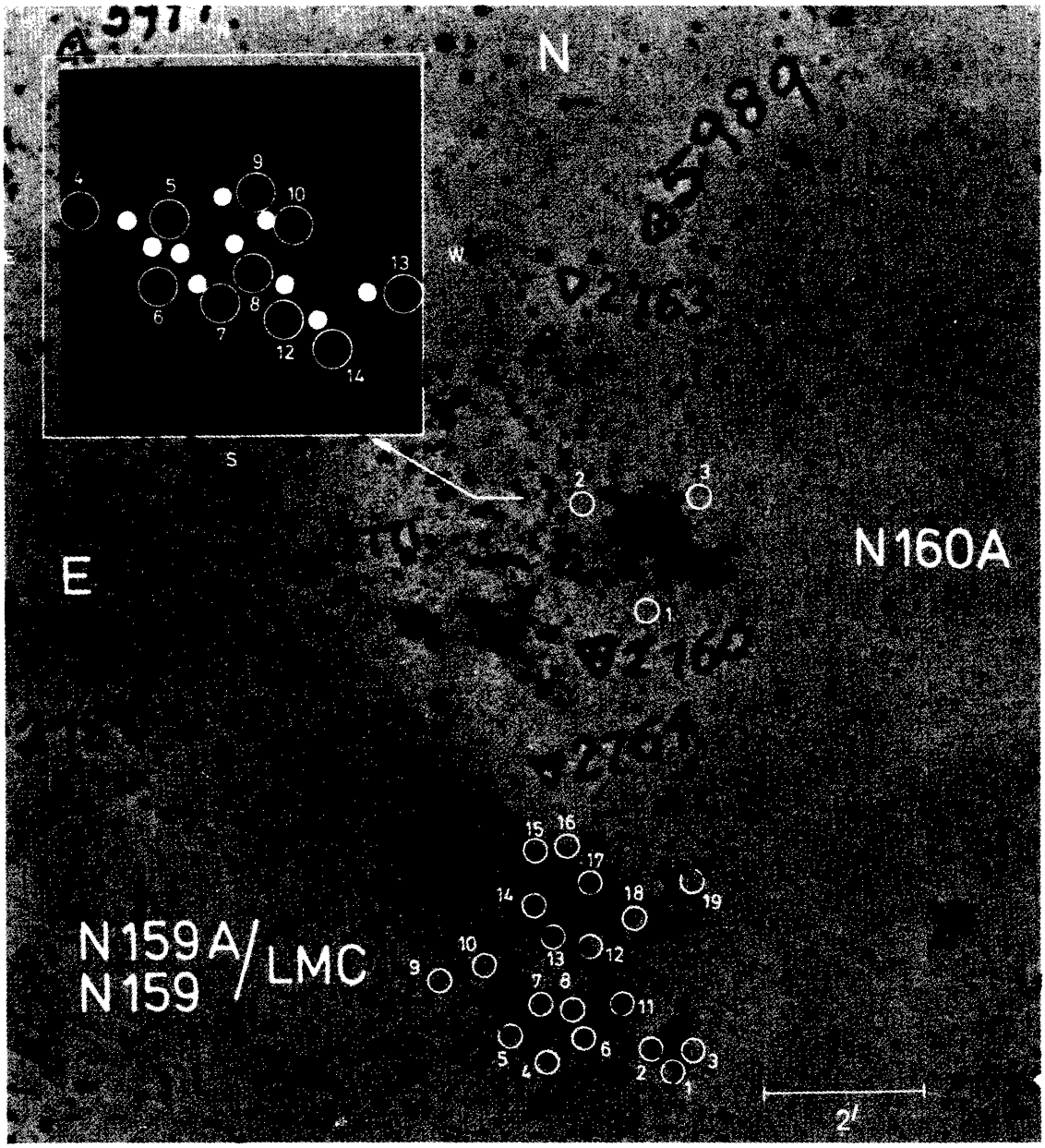

Fig. 1g. N159A, N159, N160A/LMC (from Hodge and Wright, 1967). The insert gives an enlarged view of the central region of N160A; the white dots indicate stars, drawn at the view finder

stars (generally of type OB): in $(V-B)$ the colours are more red, in $(B-U)$, $(B-L)$, $(U-W)$ the colours are more blue. In Fig. 2a we also show pure continuum colours (see Sect. 3.2) which indicate that the scatter in the colours of the EN is mainly due to line emission. Below we will return to these diagrams.

3. Calculation of colours (EN)

3.1. *VBLUW photometric system*

The *VBLUW* photometric system is described by Walraven and Walraven (1960), Rijf et al. (1969), and Lub and Pel (1977). We use the filter transmissions valid since 1980 (Lub and Pel, private communication); the effective wavelengths (λ_{eff}) and the full half widths (FHW) used in the calculations are given in Table 4. With $F(X)$ the surface flux in passband X, the colour index $(X-Y)$ is given by (see Paper I)

$$(X-Y) = \log [F(X)/F(Y)] + c(X, Y). \quad (2)$$

Table 4. Filters of the Walraven *VBLUW* (1980) system. λ_{eff} and FHW for $I(\lambda) = \text{const.}$; in A

	W	U	L	B	V
λ eff	3233	3616	3835	4277	5406
FHW	154	228	219	490	703

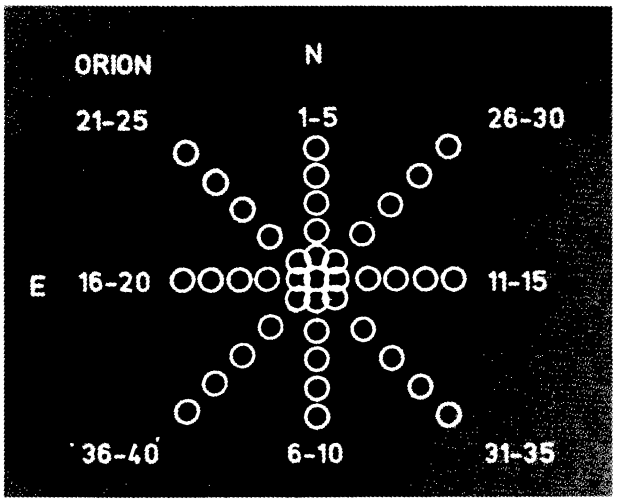

Fig. 1h. Orion nebula. The Trapezium stars are located at the center. The numbers run from the center to the outer regions

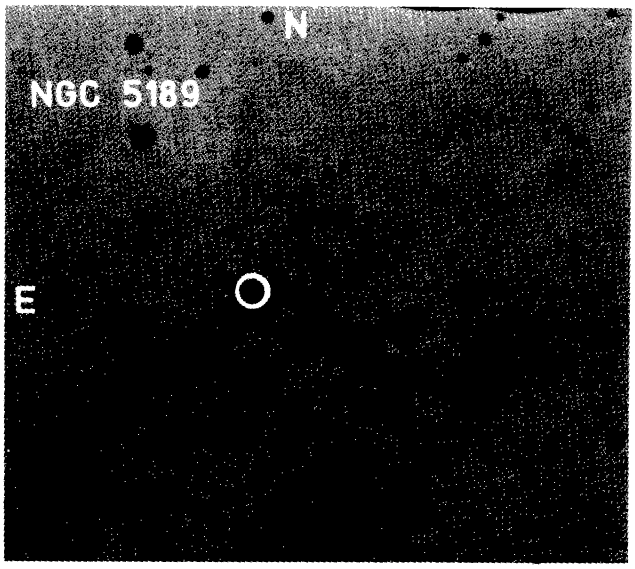

Fig. 1i. Planetary nebula NGC 5189

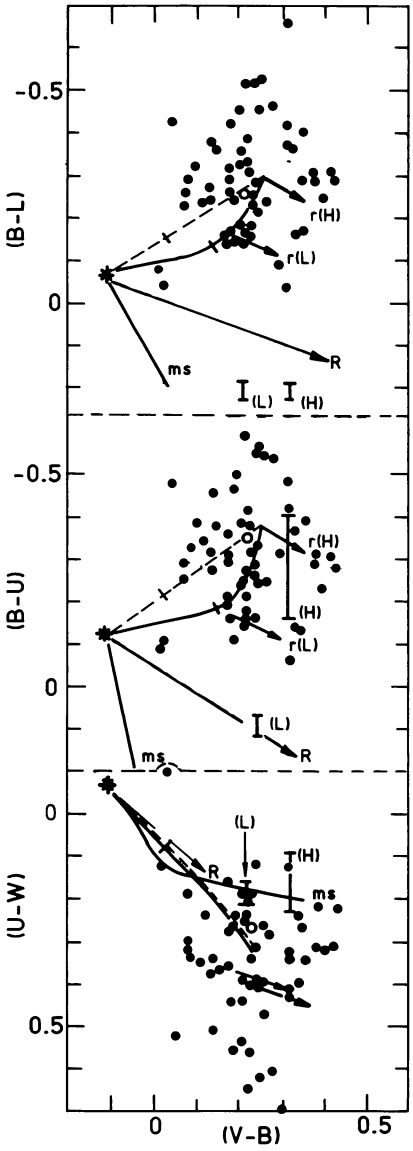

Fig. 2a. *VBLUW* colour diagrams of emission nebulae (Table 1). Solid dots: EN of the SMC, LMC; open circles: intrinsic colours of the Orion nebula (Sect. II, f2). ms: main sequence; asterisk: O 5–7 ms star; R: reddening direction. The lines starting at the O 5–7 star, running upwards, give the combined colours of the star and an EN (the ON) for decreasing brightness of the star; dashed line: star not reddened, continuous line: decrease in brightness of star due to reddening. The intersection in the lines indicate the position of equal brightness of star and EN. Arrows r(H), r(L) indicate internal reddening for high and low density EN, optically thick at endpoint of arrows. Vertical bars: pure continuum colours ($5000 < T_e < 15000$ K) for high (H) and low (L) density EN

We determined the constants $c(X, Y)$ of Eq. (2) by deriving the colours of the Sun from flux data given by Neckel and Labs (1984) and comparing the result with *VBLUW* observations of the solar type stellar analogs HD 44594, VB 64, VB 106, VB 142 (Greve and van Genderen, 1986). In the following we neglect the index $(U-W)$ because of the low accuracy due to the narrow W filter, and because only few spectroscopic observations cover the W passband.

3.2. *Emission line data*

For the calculation of colours we used emission line data of EN of the SMC and LMC taken from Dufour (1975), Dufour and Harlow (1977), Dufour and Killen (1977), Peimbert and Torres-Peimbert (1974, 1976), Pagel et al. (1978), and Dopita et al. (1981). We selected EN of the SMC and LMC because the extinction is small so that the reddening corrected line ratios are reliable. For the calculation of continua we prefer EN for which T_e has been determined (57 out of 71 data sets); in case T_e is not given we adopted $T_e = 10000$ K. The line data do not extend beyond [O II] 3727. For each EN we have completed the set of observed lines, in particular for the U and L filters, with line strengths of multiplets (for instance the H series) of which at least one member is given in the observations, using line ratios published by Osterbrock (1974) and Aller (1984). The B, U, and L passbands,

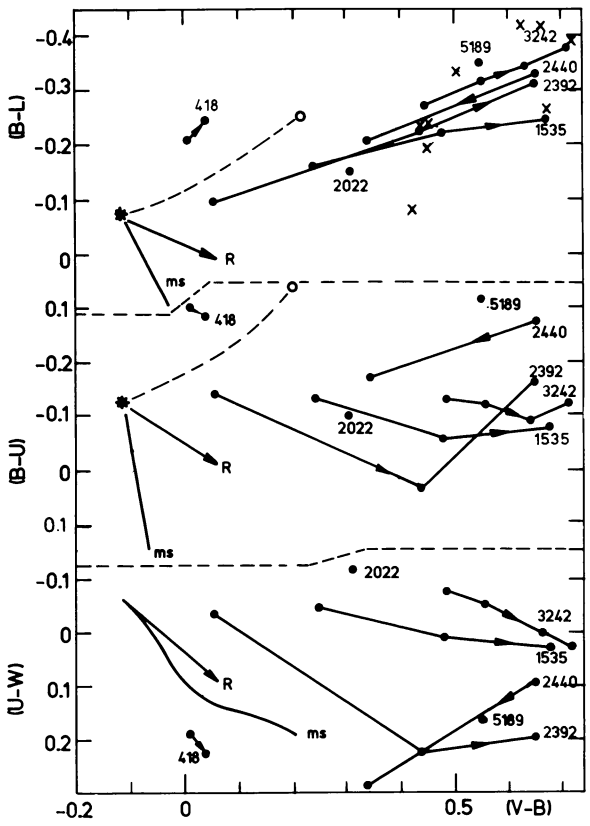

Fig. 2b. *VBLUW* diagram of planetary nebulae (Table 2). The arrows indicate increasing distance from center of PN. ms: main sequence; R: reddening direction. * indicates the combined colour of the Trapezium stars, O the colour of the Orion nebula free of scattered light. The dashed line gives the change in colour of the ON for increasing distance from the Trapezium stars, showing the influence of scattered light. x indicate calculated colours for the nebular part (emission lines + continuum) of some PN

Table 5. Flux distribution in filter passbands. L: line emission, C(2*q*): continuum emission = H(bf + ff) + 2*q*, (2*q*): 2*q* emission; all values in percent of total flux in passband

T (K)		V	B	L	U	W
Q = 0.34	HIGH DENSITY EN					
5000	C(2q)	37(12)	43(17)	12(5)	44(5)	86(13)
	L	62	57	87	56	14
10000	C(2q)	45(12)	51(16)	16(5)	40(6)	88(13)
	L	55	49	84	60	12
15000	C(2q)	43(5)	48(6)	15(2)	35(2)	86(5)
	L	57	52	85	65	14
Q = 1.0	LOW DENSITY EN					
5000	C(2q)	78(77)	84(83)	51(50)	61(60)	95(94)
	L	23	16	49	39	5
10000	C(2q)	61(57)	70(66)	33(31)	41(39)	88(83)
	L	39	30	67	59	12
15000	C(2q)	40(26)	48(33)	15(11)	22(15)	76(52)
	L	60	52	85	78	24
Number of lines in passbands, Orion spectrum (Johnson,1968) In brackets number of lines with strengths < 5 % H_β						
Number		6(10)	3(65)	9(48)	5(46)	0(6)
Flux of these lines (H_β = 1.0)		1.8	0.8	2.1	1.5	0.1
[OII]3727		-	-	~0.8	~0.8	-

which will be used later, contain on average 4–8 emission lines (see Sect. 3.4, Table 5). The influence of incompleteness of line data on calculated colours was discussed in Paper I; the corresponding uncertainty in the calculated colours is $(X-Y)<0.05$.

Line strengths of H II regions are available for several other galaxies. For NGC 6744 we use the data given by Talent (1982), for M 101 the data by Rayo et al. (1982), for 12 metal-poor galaxies the data by Kunth and Sargent (1983). However, when measuring EN in other galaxies than our own or the SMC and LMC, the observations will be most probably contaminated by an unresolved local stellar background. We discuss this effect below.

3.3. *Continua*

Except for the ON, accurate continuum observations are not available, in particular not for the SMC and LMC objects. The calculations include the H continuum (free-free and bound-free) and the 2-photon (2*q*) continuum, either for T_e or $T_e = 10\,000$ K, following the formalism given by Pottasch (1960, 1966) and Osterbrock (1974). The spectral distribution of the 2*q*-continuum is taken from Spitzer and Greenstein (1951). The strength of the 2*q*-continuum depends on the population of the H level $N(2S)$, given by Osterbrock as

$$N(2S) = N_e N_p \alpha^{\mathrm{eff}}/[A(2S,1S) + N_e q_e(2S,2P) + N_p q_p(2S,2P)]$$
$$= [N_e N_p \alpha^{\mathrm{eff}}/A(2S,1S)] \times Q \qquad (3)$$

with N_p, N_e the proton and electron density, α^{eff} the effective recombination coefficient for populating 2*S*, $A(2S,1S)$ the transition probability for 2*q*-decay, q_e and q_p the collisional transition rates for $2S \rightarrow 2P$. The numerical values of the constants are given by Osterbrock. For a low density gas $N_e \sim N_p \ll 10^4\,\mathrm{cm}^{-3}$ (for which 2*q*-decay is the main mechanism to depopulate 2*S*) we have $Q = 1.0$; for a high density gas $N_e \sim N_p \sim 3\,10^4\,\mathrm{cm}^{-3}$ (for which 2*S* can be depopulated to 2*P* by p, e collisions) we have $Q = 0.34$. In the following we will use $Q = 1.0$ and $Q = 0.34$ (see also Pottasch, 1960, 1966).

For the ratio of the Balmer continuum $I(3646)$ at $\lambda 3646$ Å, for $\Delta\lambda = 1$ Å, and the intensity $I(\mathrm{H}\beta)$ of the Hβ line we take

$$I(3646)/I(\mathrm{H}\beta) = 2.12\,T_e^{-0.673} \qquad (4)$$

as used by Simpson (1973) for the analysis of the ON. We neglect the He I and He II continua which are usually less than 10 % of the H continuum. An estimate indicates that neglecting the He continua can introduce an error $(X-Y)<0.05$ in the calculated colours.

3.4. *Sensitivity of passbands to line and continuum emission*

For different temperatures, and $Q = 1.0$, $Q = 0.34$, we give in Table 5 the flux distributions in the passbands due to calculated continua (H + 2*q*) and lines. The lines for the ON are taken from Johnson (1968). Table 5 shows that for low density EN ($Q = 1$) the

continuum is dominated by $2q$-emission, for high density EN ($Q = 0.34$) the H continuum dominates. The lines contribute a significant flux in the *VBLU* filters, however, for *W* the line contribution is only $\sim 10\%$. The continuum cannot be derived from the (absolute) *W* fluxes since the interpretation requires the knowledge of internal reddening and scattered light, i.e. the geometry of the EN. Also any colour combination $(W-X)$ is useless since the passbands $X(=V, B, L, U)$ contain too many lines. Another continuum filter in combination with *W* may solve the problem, however, such a filter cannot be incorporated into the existing photometric system. We will show below that for $(B-U)$ and $(B-L)$ the colour deviations due to internal reddening and scattered light are acceptably small in case the measurements are made sufficiently far from illuminating stars. A faint stellar background will pose a problem, see Sect. 3.7.

Below we will correlate $(B-U)$ and $(B-L)$ with the ratio [O II] 3727/Hβ. Taking the ON as a representative case, Table 5 gives the number of lines and the strength of [O II] 3727, weighted with the corresponding filter response, received in the individual passbands. Using the set of EN of the SMC and LMC (Sect. 3.2.), we find that [O II] 3727 contributes between $\sim 10\%$ (for [O II]/H$\beta \sim 1$) and $\sim 40\%$ (for [O II]/H$\beta \sim 8$) of the total fluxes in *U* and *L*. *B* does not contain [O II].

3.5. *Internal reddening*

Reddening by foreground absorption, and the corresponding corrections, are discussed in Paper I.

Gas and dust in an EN introduces absorption and reddening of the radiation passing from the inside to the surface. If we assume a homogeneous EN of volume emissivity *I* and total optical depth $\tau(V_J) = A_{V_J}/1.068$, the surface flux is

$$F(X, A_{V_J}) \propto \int I(\lambda)\,(1 - \exp(-\tau(\lambda))\,\phi_X(\lambda)\,d\lambda \qquad (5)$$

with ϕ_X the transmission function of filter *X*. We have used in Eq. (5) the extinction curve given by Savage and Mathis (1979), the emission line spectrum of the ON given by Johnson (1968), and continua for $T_e = 10\,000$ K. The colour difference between an optically thick ($F = I$) and optically thin ($F = I\tau$) nebula is $\delta(V-B) \sim 0.11$, $\delta(B-U) \sim -0.05$, $\delta(B-L) \sim -0.04$, $\delta(U-W) \sim 0.04$, independent of the value *Q*. This variation in colour is shown in Fig. 2a.

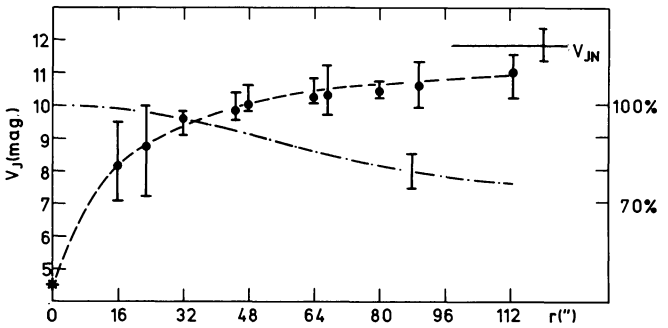

Fig. 3a. Brightness of the Orion nebula as function of distance *r* from Trapezium stars (*), not corrected for reddening. The dots give averages, the error bars peak to peak values (data of Table 1). The dashed line is the least square approximation of Eq. (6). V_{JN} is the brightness of the nebula free of scattered light. The dashed-dotted line gives the amount of scattered light, in % of the total continuum indicated at right hand scale

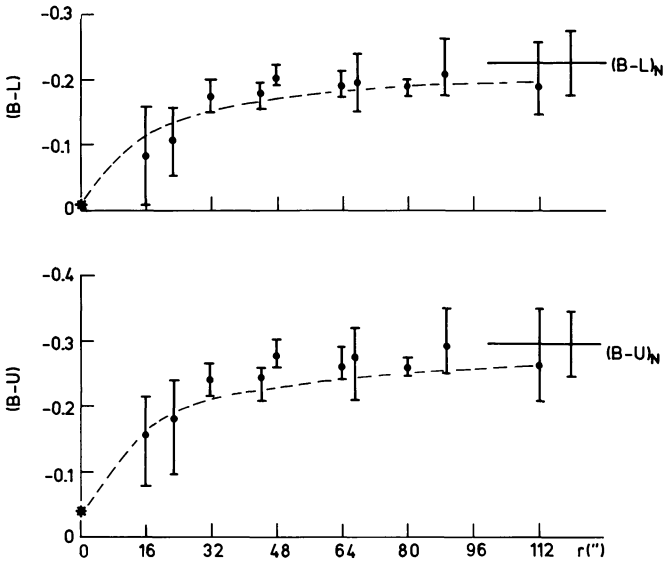

Fig. 3b. Same as Fig. 3a, for colours $(B-L)$ and $(B-U)$, not corrected for reddening (data of Table 1). $(B-L)_N$, $(B-U)_N$ indicate colours free of scattered light

3.6. *Scattered star light*

3.6.1. The Orion nebula

Observational evidence of star light scattered in the ON is given by O'Dell and Hubbard (1965), Münch and Persson (1971), Peimbert and Goldsmith (1972), Simpson (1973), Dopita et al. (1975), Schiffer and Mathis (1974), Mathis et al. (1981), and Bohlin et al. (1982). We use the *VBLUW* observations of the ON, Table 1, to estimate the influence of scattered light on the colours of EN.

Before starting the discussion of scattered light, we comment on scattered light in the atmosphere and telescope for measurements made close to a bright star. Using a diaphragm of 23″ diameter, at 30″ distance from a bright star the measured amount of scattered light is $< 1/1000$ of the stellar flux, for all passbands. Since the brightness of the Trapezium stars is $V_J = 4.6$ mag, at 30″ distance the "instrumental" scattering is $V_{J,S} > 13$ mag. This effect is unimportant in the following analysis (see Fig. 3a and 3b).

Figure 3a shows the observed magnitudes V_J, per $(200'')^2$, of the ON as function of distance *r* from the Trapezium stars (Table 1). At 550 pc distance, the angular increments of 16″ in Fig. 3a (3b) are equal to 0.04 pc. The decrease in brightness V_J with increasing *r* as exhibited in Fig. 3a is due to the decrease in the amount of scattered light and the decrease in brightness of the nebula in the outer regions. We use the Hβ map published by Dopita et al. (1975) to estimate the decrease in brightness of the nebula. We may assume that the intensities *V*, *B*, *L*, *U*, *W*, and V_J change in a similar way as Hβ. Then, from the variation of Hβ with *r* we estimate that between $r \sim 0''$ and $r \sim 120''$ the change in V_J is $\Delta V_J \sim 1$–1.5 mag. This change in brightness is much smaller than the observed change, being of the order of 5–6 mag between $r \sim 0''$ and $r \sim 120''$. Hence we interpret the decrease in V_J as exhibited in Fig. 3a as mainly due to scattered light. We approximated the observations of Fig. 3a by the empirical function

$$V_J(r) = V_J(*) + V_{J0}(1 - 1/(1 + r)) \qquad (6)$$

with $V_J(r)$ the observed magnitude at distance r, $V_J(*)$ the magnitude of the 4 Trapezium stars given in Table 3, and V_{J0} a constant. The least square solution of Eq. (6), representing a homogeneous nucleus of the nebula, is shown in Fig. 3a. For large r the observations approach the true brightness of the nebula $V_{JN} \approx V_J(*) + V_{J0}$, i.e. the brightness free of scattered light which we call "intrinsic" brightness. Adopting a foreground extinction of $A_{V_J} = 0.75$ mag (Sect. 2), at $r \sim 120''$ we find $V_{JN} \approx (11 \pm 0.5)$ mag per $(200'')^2$.

In a similar way we approximated the fluxes observed in the individual *VBLUW* passbands

$$\log F(X,r) = \log F(X,*) + (1 - 1/(1+r)) \log F(X_0). \quad (7)$$

From the least square solutions of Eq. (7) we calculated the colours $(X-Y)_{N+S}$ of the nebular emission plus scattered light as function of r. Figure 3b shows the observed $(B-L)$, $(B-U)$ and calculated $(B-L)_{N+S}$, $(B-U)_{N+S}$. For large r we obtain the intrinsic fluxes of the nebula $F(X)_N = F(X,*)\,F(X_0)$ from which we derived the intrinsic colours at $r \sim 120''$, indicated $(B-L)_N$, $(B-U)_N$ in Fig. 3b. The nebula may be somewhat more blue, but hardly more red, than $(B-L)_N$, $(B-U)_N$.

We checked whether the predictions from the approximations are consistent with the observations by Simpson (1973). Using the reddening corrected line strengths and continuum (atomic + scattered) intensities measured by Simpson at ~ 80–$150''$ distance from the Trapezium stars (slit positions 1, 2, 3) we derive $(V-B)_{SIM} = 0.22$, $(B-U)_{SIM} = -0.38$, $(B-L)_{SIM} = -0.26$. Using the functions $F(X,r)$ of Eq. (7), and applying a reddening correction $A_{V_J} = 0.75$ mag, for position $r \sim 120''$ we obtain $(V-B)_{120} = 0.19$, $(B-U)_{120} = -0.32$, $(B-L)_{120} = -0.24$, in agreement with the colours derived from Simpson's data. Using the line to continuum ratios in the passbands given in Table 5, and $F(X, r=120)/F(X)_N$, we find that at position $r \sim 120''$ the continuum contains $\sim 75\,\%$ scattered light, in agreement with the observations by Simpson (1973) and O'Dell and Hubbard (1965). In a similar way we derived from $F(X,r)/F(X)_N$ the amount of scattered light as function of r, shown in Fig. 3a.

3.6.2. Colour corrections for scattered light

Using the values $F(X)_N$ of Eq. (7), the intrinsic, reddening corrected colours of the ON are $(V-B)_N = 0.23$, $(B-U)_N = -0.35$, $(B-L)_N = -0.26$ with an estimated accuracy of $|0.05|$ to $|0.03|$. At position $r \sim 120''$, where the continuum contains $\sim 75\,\%$ scattered light, the colour corrections $\Delta(X,Y)$ defined as

$$(X-Y)_N = (X-Y)_{N+S} + \Delta(X,Y) \quad (12)$$

are $\Delta(V,B) \sim 0.04$, $\Delta(B,U) \sim -0.03$, $\Delta(B,L) \sim -0.02$.

The observations of the EN in the SMC and LMC are made at distances $> 16''$, i.e. at distances > 5 pc, from nearby stars brighter than $V_J \sim 15$ mag, i.e. $M_{V_J} < -3$ mag. Extrapolating from the ON, for which the observations extend to ~ 0.3 pc and for which the combined brightness of the Trapezium stars is $M_{V_J} \sim -4$ mag, for the EN of the SMC and LMC we may expect negligible influence of scattered light on the observed colours.

3.7. *Stellar background*

With the eyepiece equipment of the Dutch telescope we are able to see stars brighter than $V_J \sim 15$ mag. Inspecting deeper photographs of the SMC and LMC (Hodge and Wright, 1967, 1977; ESO Sky Atlas), we avoided measurements of EN at places where stars of magnitudes $V_J \lesssim 18$ mag are located. However, the measurements of the EN may include stars of $V_J \gtrsim 18$–19 mag. In Fig. 2a we show the combined colour of a typical EN (the ON) and an O 5–7 ms star. Depending on the brightness of the star, the combined colour lies on the indicated tracks. Assuming an EN of $V_J = 16$ mag per $(200'')^2$ and an O 5–7 ms star of $V_J = 18$ mag, the deviation of the combined colour from the intrinsic nebular colour is $\delta(V-B) \sim 0.06$, $\delta(B-U) \sim \delta(B-L) \sim 0.04$.

We are certain that for most of the measurements of the SMC and LMC objects the influence of low brightness stars is negligible. However, as evident from Fig. 2a, measurements of EN in other galaxies are difficult unless the EN are isolated from the stellar background.

4. Agreement of calculations and observations (EN)

4.1. *The Orion nebula*

We give in Table 6 the reddening corrected, intrinsic colours (free of scattered light) of the ON derived in Sect. 3.6.1. These colours are compared with calculated colours, also given in Table 6, using the line data given by Johnson (1968) and using either the reddening corrected continuum measured by Simpson (1973, slit

Table 6. Observations and predictions for the Orion nebula (redden. corr.)

	V-B	B-U	B-L	
1) Extrapolated from Eq.(7)	0.23(0.05)	-0.35(0.03)	-0.26(0.03)	
2) Lines (Johnson,1968) + continuum from Simpson(1973)	0.22(0.01)	-0.38(0.01)	-0.26(0.01)	
3) same as 2), corrected for 75 % scattered light	0.26(0.02)	-0.41(0.01)	-0.28(0.01)	
4) Lines (Johnson,1968) + contin. for T_e= 8700 K				nebula
high density gas(Q=0.34)	0.36	-0.33	-0.25	opt. thick
	0.26	-0.38	-0.29	opt. thin
5) Lines (Johnson,1968) + contin. for T_e= 8700 K				
low density gas(Q=1.0)	0.29	-0.09	-0.09	opt. thick
	0.18	-0.15	-0.13	opt. thin

Values in brackets give estimated accuracy

position 1, 2, 3) and corrected for scattered light (Sect. 3.6.1.), or using theoretical continua for $T_e = 8700$ K as derived by Simpson. We give the colours for a low density ($Q = 1.0$) and high density ($Q = 0.34$) gas representing approximately two possible components of the ON (cf. Simpson, 1973). The comparison seems to indicate a high density component.

4.2. *Other emission nebulae*

As evident from Sect. 2 and 3, only a statistical comparison can be made between the set of observations and calculations covering a variety of physical states of EN (T_e, N_e, abundance), implicitly given by the line ratios.

Figure 2a shows the observed colours in the commonly used CDs. The scatter is large because of the broad V passband, and the large number of lines therein (see Table 5), and the narrow W passband for which the observations ($U-W$) are not very accurate. However, the situation is different for the CD ($B-U$)/($B-L$) shown in Fig. 4. A systematic distribution of the observed and calculated colours is noticed and, on a statistical basis, we find agreement between the observations and the calculations. The calculated colours of the EN in NGC 6744 and M101 (Sect. 3.2.) are similar; however, the calculated colours of the metal-poor EN (Sect. 3.2.) seem to be more red, a fact which merits further observational investigations. In Fig. 4 we show the main sequence branch and there exists no confusion between nebular and stellar objects, except for a region at the red part of the nebular colours which seems to be occupied by metal-poor EN.

5. Correlation (B–U) – [O II] 3727/Hβ for EN

The systematic distribution of the colours in the CD ($B-U$)/($B-L$), Fig. 4, is mainly produced by emission lines received in the corresponding passbands. This conclusion is obtained from the fact that the continuum colours (i.e. the unrealistic case of no emission lines) for $5000 < T_e < 15\,000$ K are restricted to isolated and narrow regions in the CD of Figs. 2 and 4. This result made us search for a correlation of the calculated (and observed) colours with the strengths of dominant emission lines; a useful correlation was found for [O II] 3727.

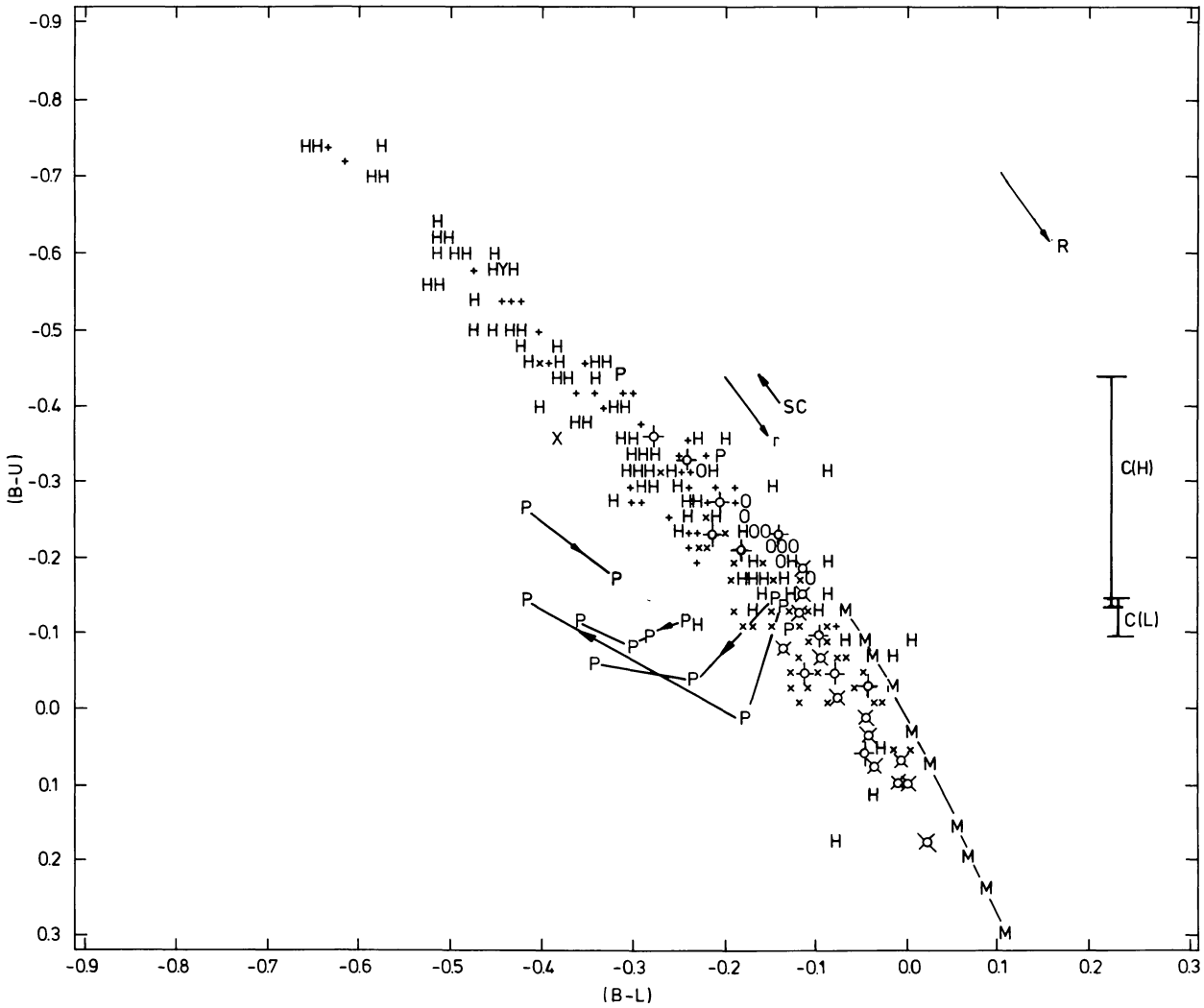

Fig. 4. ($B-U$)/($B-L$) diagram of observed and calculated colours of EN. Observations: H are EN of the LMC, SMC; O is the Orion nebula, P are planetary nebulae (arrows indicate increasing distance from center). X: SNR N49 (LMC), Y:SNR RCW86 (Greve et al., 1982). Calculations: + high density EN ($Q = 0.34$), × low density EN ($Q = 1.0$). ⊹ ⌑ idem for metal-poor EN. Vertical bars denote pure continuum colours (no lines) for $5000 < T_e < 15\,000$ K and high (H) and low (L) density gas. R: reddening for $A_{V_J} = 1.0$ mag.; r: influence of internal reddening (optically thick at endpoint of arrow); SC: influence of scattered light (75% for ON); also evident in the scatter of the Orion observations. The main sequence is indicated by the points M and the dashed line, starting with an O 5–7 star

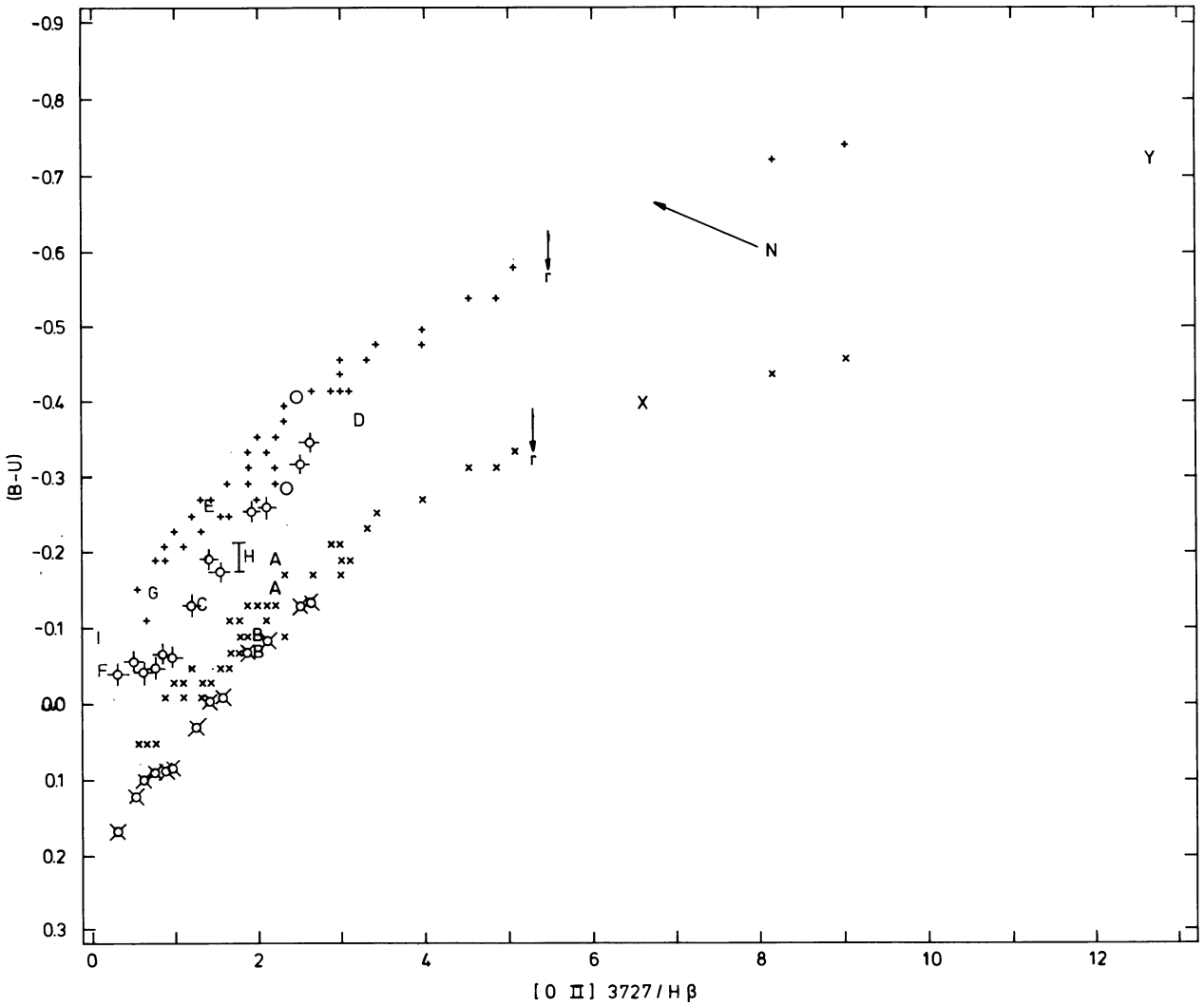

Fig. 5. *VBLUW* system. Predicted correlation $(B-U)$ with [O II] 3727/Hβ for high density EN: +, for low density EN: ×, ⊹ ⌑ idem for metal-poor EN. Observations: A: N 83A, B(LMC); B: NGC 2077 (LMC); C: NGC 2080 = N 160A (LMC); D: N 11E (LMC); O: Orion Nebula; N: N 70 (LMC); X: SNR N 49 (LMC); Y: SNR RCW 86 (Galaxy); E: IC 418; F: NGC 1535, NGC 2022; G: NGC 2392; H: NGC 2440; I: NGC 3242; reddening corrected data. The arrow illustrates the influence of $A_{V_J} = 0.6$ mag extinction for N 70. r: influence of internal reddening (optically thick at endpoint of arrow)

The [O II] 3727 lines are favourably located in the *U*, *L* passbands, see Table 5. In Fig. 5 we show the correlation $(B-U)$ with [O II] 3727/Hβ; the correlation $(B-L)$ – [O II] 3727/Hβ is similar. The correlation is good and there exists also a useful dynamic range [i.e. $\Delta(B-U) \sim 0.7$ for Δ[O II]/H$\beta \sim 10$] since observations of the brighter nebulae ($V_J < 14$–15 mag for 15–20″ diaphragm) can be made with an accuracy of $\delta(B-U) \sim |0.02|$. Figures 4 and 5 indicate a separation between low density and high density EN, and normal and metal-poor EN. When using the correlation of Fig. 5, there exists an ambiguity between low density and high density nebulae; however, we notice in Fig. 4 that the corresponding nebulae cluster in different regions of the CD which may be used as a coarse indication of the particular case. For $(B-U) > -0.1$ confusion may arise between stars and (compact) EN.

At present we have only few observations which, however, seem to confirm the correlation; the data are plotted in Fig. 5. Estimates of [O II] 3727/Hβ for the EN denoted in Fig. 5 by A–D are taken from Kaler (1976) and the references given in Sect. 3.2.; however, there exists the uncertainty of the positions where the spectroscopic data are obtained. The nebula O of Fig. 5 is the ON at positions where the photometric data approximately correspond with the observations by Reitmeyer (1965). The nebula N of Fig. 5 is N 70 of the LMC. The photometric data are obtained at the brightest part of the shell region (Greve and van Genderen, 1985), the corresponding spectroscopic data are given by Dopita et al. (1981). This extreme point in Fig. 5 substantiates the predicted correlation.

Earlier we (Greve et al., 1982) obtained *VBLUW* colours of the supernova remnants RCW 86 and N49 of which good spectroscopic data are available from Ruiz (1981), and Osterbrock and Dufour (1973), respectively. Adopting for RCW 86 an extinction of $A_{V_J} = 0.8$ mag (Ruiz, 1981), the values shown in Fig. 5 seem to confirm the correlation.

6. The planetary nebulae

For the PN, usually being high density nebulae (cf. Torres-Peimbert and Peimbert, 1977; TPP, 1977) with reduced $2q$-continuum (see Sect. 3.3), the observed fluxes consist of the stellar continuum if the star is located in, or very close to, the diaphragm, the nebular continuum (mainly H: ff + bf), emission lines, and scattered light.

6.1. Position of the PN in the CDs

Figure 2b shows the observations of the PN in the commonly used CDs. This figure shows that the further away from the central star the observations are made, the redder is $(V-B)$, approaching at the largest distances the "true" nebular colours. Exceptions are IC 418, which is a compact ($\sim 10''$ diameter, cf. Reay and Worswick, 1978) low ionization object (TPP, 1977), and NGC 2440, which contains a large amount of dust (cf. Calvet and Peimbert, 1983). To substantiate the observed nebular colours, we show in Fig. 2b for some bright PN calculated colours $(V-B)$, $(B-L)$ using line data collected by Kaler (1976) and T_e values taken from the literature. We notice that, statistically, the calculated colours agree with the observations of the nebular part. Observations made close to, or including the central star contain the stellar continuum of colour $(V-B) \sim (B-L) \sim -0.1$ for OB type stars, so that the combined colour of the nebula and the stellar continuum moves to bluer values $(V-B)$. A similar effect is illustrated in Fig. 2a, 2b for the combined colours of the ON and the Trapezium stars.

The V filter contains the dominating [O III] 4959, 5007 emission lines (TPP, 1977), with $\sim 30\%$ transmission at 5000 Å; the B filter does not contain strong lines. We expect $(V-B)$ to be more red the stronger [O III] is. IC 418 is a low excitation nebula with [O III]/H$\beta \sim 1.7$, the other nebulae are high excitation nebulae with [O III]/H$\beta \sim 10$–15 (TPP, 1977). Hence, we observe in Fig. 2b that IC 418 is more blue than the other nebulae.

Reflection nebulae appear more blue than the illuminating star, with the outer parts of a nebula usually more blue than the

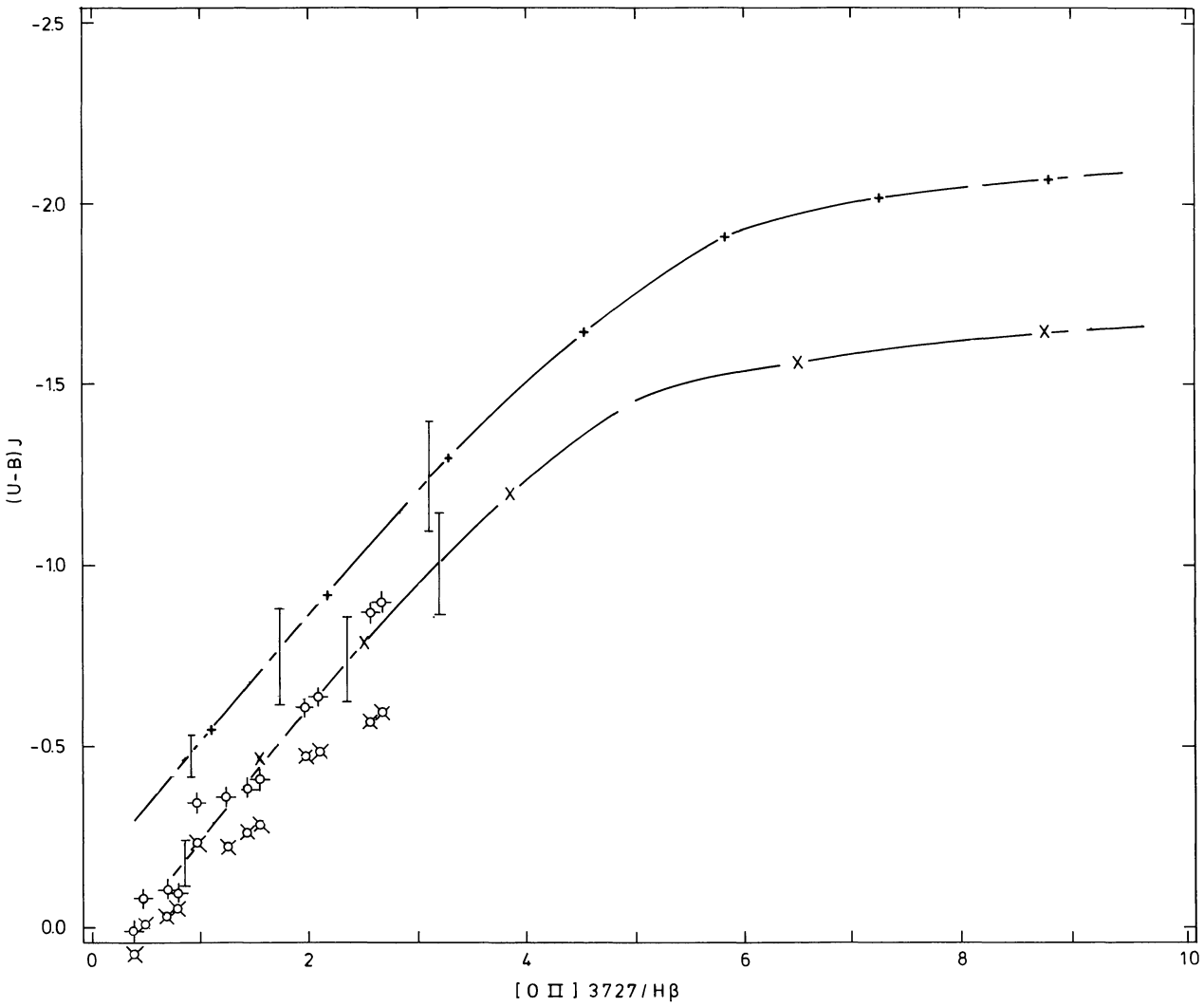

Fig. 6. *UBV* system. Predicted correlation $(U-B)_J$ with [O II] 3727/Hβ for high density EN: —— + —— + ——, for low density EN: —— × —— × ——. The error bars give the variation in $(U-B)_J$ for given [O II]/Hβ as derived from the set of data explained in Sect. 3. ⊹ ⊠ idem for metal-poor EN

central parts (cf. Witt, 1985; de Oliveira and Maciel, 1986). This effect of light scattering seems to dominate in the outer parts of the dusty nebula NGC 2440, see Fig. 2b.

6.2. *Correlation* $(B-U)$ – [O II] 3727/Hβ *for PN*

Knowing from a) that at the largest distances the colours are mainly due nebular emission, in Fig. 5 we show the correlation of $(B-U)$ with [O II]/Hβ. The values [O II]/Hβ are taken from TPP (1977), the values $(B-U)$ are those for the largest off-center measurements (Table 2). The corresponding positions in Fig. 5 follow the high density region (except NGC 2440, see above), as to be expected; adding further confidence in the predicted correlation.

7. Other photometric systems

In a similar way we have investigated the Johnson *UBV*, the Stromgren *uvby* and the Geneva systems (cf. Lamla, 1982). As shown in Fig. 6, the $(U-B)_J$ index of the *UBV* system shows some correlation with [O II] 3727/Hβ, however, the scatter is large compared to Fig. 5. This is mainly due to the fact that the U_J, B_J filters have approximately twice the widths of the *U*, *B* filters, and hence contain more lines and correspondingly exhibit more fluctuations in the integrated line intensities. Also, B_J includes Hβ which is nearly excluded in *B*. The variation in $(U-B)_J$ for constant [O II]/Hβ due to this fluctuation in line intensities, as derived from the data explained in Sect. 3, is shown by the error bars in Fig. 6.

A useful correlation with [O II] 3727/Hβ is also found for the Stromgren index $(u-b)$; we found no correlation for the Geneva system.

Since [O III] 4959, 5007 is strong in EN, we have searched for a correlation with relevant colour indices of the *VBLUW*, *UBV*, *uvby* systems. No useful correlations are found which is attributed to the fact that [O III] is located in the broad *V*, *v* filters which contain many lines.

8. Conclusion

Using the Orion nebula as a representative case we discussed the influence of internal reddening and scattered light on the intrinsic colour of an EN. In case the observations are made sufficiently far from illuminating stars, and in case confusion with a stellar background can be avoided, as was done in the observations of the SMC and LMC objects, the measurements give sufficiently accurate intrinsic colours. We have shown that calculations using line ratios and the H and 2-photon continuum can reproduce the colours of EN in the $(B-U)/(B-L)$ diagram, see Fig. 4. This agreement, though on a statistical basis, of the calculated and observed $(B-U)$, $(B-L)$ indices gives confidence in the predicted correlation of $(B-U)$ with [O II] 3727/Hβ, see Fig. 5. At present, this correlation seems to be confirmed by a few observations of EN and PN available. If verified by further observations, this correlation may be used as a diagnostic indicator of H II regions and PN.

Acknowledgements. We are indebted to Dr. J. Lub who made the computer programs for various parts of the automatic data reduction. We appreciated the comments of the referee which stimulated a deeper investigation of the observations and interpretation.

References

Aller, L.H.: 1984, *Physics of Thermal Gaseous Nebulae*, Reidel, Dordrecht
Bohlin, R.C., Hill, J.K., Stecher, T.P., Witt, A.N.: 1982, *Astrophys. J.* **255**, 87
Calvet, N., Peimbert, M.: 1983, *Rev. Mexicana Astron. Astrofis* **5**, 319
de Oliveira, M. Maciel, W.J.: 1986, *Rev. Mexicana Astron. Astrofis.* **12**, 273
Dopita, M.A., Isobe, S., Meaburn, J.: 1975, *Astrophys. Space Sci.* **34**, 91
Dopita, M.A., Ford, V.L., McGregor, P.J., Mathewson, D.S., Wilson, I.R.: 1981, *Astrophys. J.* **250**, 103
Dufour, R.J.: 1975, *Astrophys. J.* **195**, 315
Dufour, R.J., Harlow, W.V.: 1977, *Astrophys. J.* **216**, 706
Dufour, R.J., Killen, R.M.: 1977, *Astrophys. J.* **211**, 68
Gathier, R.: 1984, *A Study of Planetary Nebulae*, Thesis, Groningen
Gathier, R., Pottasch, S.R., Pel, J.W.: 1986, *Astron. Astrophys.* **157**, 171
Goudis, C.: 1982, *The Orion Complex*, Reidel, Dordrecht
Greve, A., van Genderen, A.M.: 1982, *Astron. Astrophys.* **111**, 185 (Paper I)
Greve, A., van Genderen, A.M.: 1985, *Astron. Astrophys.* **148**, 397
Greve, A., van Genderen, A.M.: 1986, *Astron. Astrophys.* **160**, 392
Greve, A., van Genderen, A.M., Dennefeld, M., Danziger, I.J.: 1982, *Astron. Astrophys.* **111**, 171
Henize, K.G.: 1956, *Astrophys. J. Suppl.* **2**, 315
Hodge, P.W., Wright, F.W.: 1967, *The Large Magellanic Cloud*, Smithsonian Institution Astrophys. Obs., Smithsonian Press
Hodge, P.W., Wright, F.W.: 1977, *The Small Magellanic Cloud*, University of Washington Press, Seattle
Johnson, H.M.: 1968, *Diffuse Nebulae*, in Nebulae and Interstellar Matter, *Stars and Stellar Systems Vol.* **II**, eds. B.M. Middlehurst, L.H. Aller, Univ. Chicago Press, p. 65
Kaler, J.B.: 1976, *Astrophys. J. Suppl.* **31**, 517
Kunth, D., Sargent, W.L.W.: 1983, *Astrophys. J.* **273**, 81
Lamla, E.: 1982, in *Landolt-Börnstein, Vol. 2*, eds. K. Schaifers, H.H. Voigt, Springer, Berlin, Heidelberg, New York, p. 35
Laval, A., Greve, A., van Genderen, A.M.: 1986, *Astron. Astrophys.* **164**, 26
Lub, J., Pel, J.W.: 1977, *Astron. Astrophys.* **54**, 137
Mathis, J.S., Perinotto, M., Patriarcchi, P., Schiffer, F.H.: 1981, *Astrophys. J.* **249**, 99
Münch, G., Persson, S.E.: 1971, *Astrophys. J.* **165**, 241
Neckel, H., Labs, D.: 1984, *Solar Phys.* **90**, 205
O'Dell, C.R., Hubbard, W.B.: 1965, *Astrophys. J.* **142**, 591
Osterbrock, D.E.: 1974, *Astrophysics of Gaseous Nebulae*, Freeman, San Francisco
Osterbrock, D.E., Dufour, R.J.: 1973, *Astrophys. J.* **185**, 441
Pagel, B.E.J., Edmunds, M.G., Fosbury, R.A.E., Webster, B.L.: 1978, *Monthly Notices Roy. Astron. Soc.* **184**, 569
Pagel, B.E.J., Edmunds, M.G., Blackwell, D.E., Chun, M.S., Smith, G.: 1979, *Monthly Notices Roy. Astron. Soc.* **189**, 95
Peimbert, M., Torres-Peimbert, S.: 1974, *Astrophys. J.* **193**, 327
Peimbert, M., Torres-Peimbert, S.: 1976, *Astrophys. J.* **203**, 581
Peimbert, M., Goldsmith, D.W.: 1972, *Astron. Astrophys.* **19**, 398
Pel, J.W.: 1983, Internal Report, Leiden
Pottasch, S.R.: 1960, *Ann. Astrophys.* **23**, 749
Pottasch, S.R.: 1966, in *Vistas Astron. Vol.* **6**, ed. A. Beer, Pergamon Press, p. 149

Pottasch, S.R.: 1984, *Planetary Nebulae*, *Astrophys. Space Sci. Library* **107**, Reidel, Dordrecht
Rayo, J.F., Peimbert, M., Torres-Peimbert, S.: 1982, *Astrophys. J.* **255**, 1
Reay, N.K., Worswick, S.P.: 1978, *Astron. Astrophys.* **179**, 31
Reitmeyer, W.L.: 1965, *Astrophys. J.* **141**, 1331
Rijf, R., Tinbergen, J., Walraven, Th.: 1969, *Bull. Astron. Inst. Netherlands* **20**, 279
Ruiz, M.T.: 1981, *Astrophys. J.* **243**, 814
Savage, B.D., Mathis, J.S.: 1979, *Ann. Rev. Astron. Astrophys.* **17**, 73
Schiffer, F.H., Mathis, J.S.: 1974, *Astrophys. J.* **194**, 597
Shaver, P.A., McGee, R.X., Newton, L.M., Danks, A.C., Pottasch, S.R.: 1983, *Monthly Notices Roy. Astron. Soc.* **204**, 53
Simpson, J.P.: 1973, *Publ. Astron. Soc. Pacific* **85**, 479
Spitzer, L., Greenstein, J.L.: 1951, *Astrophys. J.* **114**, 407
Stasińska, G.: 1980, *Astron. Astrophys.* **84**, 320
Talent, D.L.: 1982, *Astrophys. J.* **252**, 594
Torres-Peimbert, S., Peimbert, M.: 1977, *Rev. Mexicana Astron. Astrofis.* **2**, 181
Walraven, Th., Walraven, J.H.: 1960, *Bull. Astron. Inst. Netherlands* **15**, 67
Witt, A.N.: 1985, *Astrophys. J.* **294**, 216